Journal of Applied Polymer Science

Solid state polymerization in a micro-reactor: The case of poly(tetramethylene terephthalamide)

Constantine D. Papaspyrides,[1] Athanasios D. Porfyris,[1] Stamatina Vouyiouka,[1] Ruud Rulkens,[2] Eric Grolman,[2] Geert Vanden Poel[2]

[1]Laboratory of Polymer Technology, School of Chemical Engineering, National Technical University of Athens, Athens 15780, Greece

[2]DSM Ahead B.V, Geleen 6167, The Netherlands

Correspondence to: C. D. Papaspyrides (E-mail: kp@cs.ntua.gr)

ABSTRACT: The aim of this work was to develop and optimize a direct solid state polymerization (DSSP) process on a micro scale for alkyldiammonium-terephthalate salts. This was successfully demonstrated for the first time by the case of tetramethylenediammonium-terepthalate salt (4T salt). The derived polymer (PA4T) presents interesting properties, but the temperature-favored acid catalyzed cyclization of tetramethylenediamine (TMD) to mono-functional pyrrolidine and ammonia inhibits a high polymerization conversion. DSSP was performed in a thermogravimetrical analysis (TGA) chamber, and the continuously monitored weight loss was correlated to polymerization conversion via the release of water, excluding any mass and heat transfer limitations. It was found that the conditions under which the DSSP is performed and the morphology of the starting material affect both the reaction rate and the product quality. The effect of the critical process parameters, namely vent size, heating rate to reach SSP temperature, and reaction temperature were quantified by the observed mass loss and by ^{1}H NMR analysis. It was noticed that, besides the water formed by amidation, other volatile compounds were also released during the DSSP reaction, with main component, the TMD. In particular, it was observed that conditions favoring the evaporation of TMD also favored a higher reaction rate. The TMD loss was minimized by optimization of the aforementioned process conditions, leading to a more thermally stable and a higher molecular weight final product. The thermal stability of the PA4T was found to be inversely correlated to the concentration of carboxylic end groups present in the formed polymer. © 2015 Wiley Periodicals, Inc. J. Appl. Polym. Sci. **2016**, *133*, 43271.

KEYWORDS: polyamides; synthesis and processing; thermogravimetric analysis (TGA)

Received 26 August 2015; accepted 24 November 2015

DOI: 10.1002/app.43271

INTRODUCTION

Polyamides (PAs) are engineering thermoplastics with a wide variety of industrial and commercial end uses. PAs can be classified into (a) aliphatic polyamides made from α,ω-amino-acids or from aliphatic diamines and aliphatic diacids, e.g. poly(caproamide) (PA 6) or poly(hexamethylene adipamide) (PA 66), (b) aramides having 85% or more of the amide groups directly connected to two aromatic groups, and (c) semi-aromatic polyamides, such as PA XT, in which terephthalic acid (TA) is the dicarboxylic acid.[1–4]

With increasingly stringent requirements in for example the automotive and electronics industries, applications of aliphatic polyamides are declining because of their poor dimensional stability and limited thermal properties. On the other hand, aromatic polyamides, such as poly(*p*-phenylene terephthalamide) and poly(*m*-phenylene isophthalamide), are considered to be high-performance materials due to their superior thermal and mechanical properties. However, they exhibit extremely high melting temperatures that lie above their decomposition points, requiring special methods for their processing.[5–8] To combine the high melting temperatures and heat resistance of aromatic PAs with the melt processability of aliphatic ones, semi-aromatic polyamides developed rapidly in the past 20 years,[8,9] with commercially available grades of poly(hexamethylene terephthalamide) (PA 6T) copolymers, such as Ultramid T (BASF) (PA6T/6 copolymer with 6 = caprolactam) and Zytel HTN 51 (DuPont) (PA6T/DT, copolymer with *D* = 2-methyl pentamethylene diamine).[2,8]

Regarding polymerization routes of the terephthalate-based (co)polyamides, a melt process is often problematic or even impossible, (e.g., PA6T, $T_m \approx 375$°C).[1,4] The most common polymerization methods are the reaction of diacid dichlorides with diamines at low temperatures or direct condensation

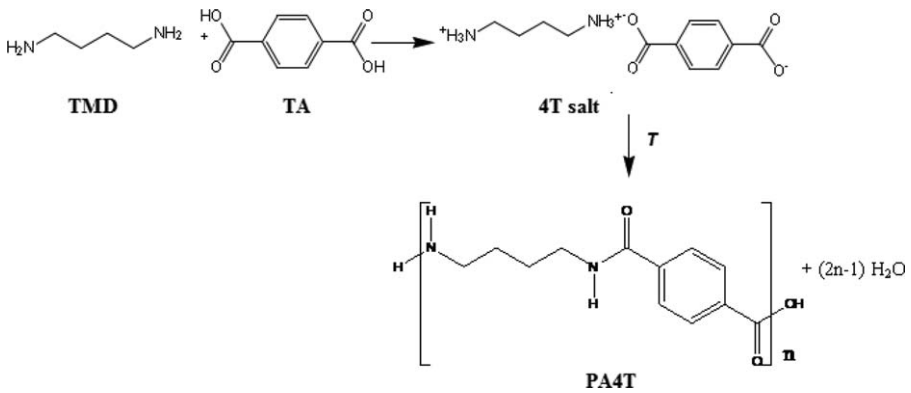

Figure 1. Synthesis and polycondensation reaction of 4T salt.

reactions in solution of aromatic diacids with diamines at high temperatures.[5] Further increase of molecular weight can be achieved through applying a post solid state polymerization (post-SSP) step on a low-molecular-weight prepolymer. Post SSP is widely applied in industry for the production of aliphatic polyamides and thermoplastic polyesters (e.g., PET, PBT).[10–12] It has been also studied for the synthesis of PA 4T,[13] PA 4I,[14] co-polyamides PA 46/4T,[15] PA 4T/6T,[16] and terpolyamides.[17,18] In a recent publication,[19] the effect of prepolymer properties (particle size and aromatic diacid composition) and SSP parameters (temperature, time, sweep gas flow rate, and steam content of the sweep fluid) was thoroughly studied for the post SSP of PA 4T/46.

Solid state polymerization has been also investigated directly on polyamide monomers (direct SSP, DSSP), avoiding the high temperatures associated with melt technology and minimizing side reactions and thermal degradation.[20–23] Polyamides are unique in the sense that the monomers are a combination of amine base and carboxylic acid groups, hence they crystallize as salts. Accordingly, the monomers can often be transformed into a polymer at a temperature lower than both the melting point of the salt and the polymer, under flowing nitrogen, vacuum, or high pressure[24–29]; in many cases, the reactions are topotactic and the monomer crystals can be converted into polycrystalline polymer aggregates, permitting the preparation of highly oriented polymers.[28,29] Regarding aliphatic polyamide structures, examples involve the DSSP of salts for the preparation of PA 26,[30] PA 210,[30] PA 46,[27,30] PA 66,[20,23–25,27,28,31] PA 610,[24,27] PA 126,[25,30] PA 1210.[24,27] In the case of aminoacids, zwitterionic starting materials have been ε-aminocaproic acid for PA 6,[32] aminoenanthoic (PA 7), aminoperlagonic (PA9), and aminoundecanoic (PA11) acid.[33,34] Regarding aramides, 4-amino-4″-carboxy-*p*-terphenyl acid[35,36] and phenoxycarbonyl-*a*-amino acid[37] were solid state polymerized resulting in poly[4,4″(*p*-terphenylene)amide] and poly(*p*-benzamide), respectively. In a recent study,[38] the successful direct synthesis in the solid state of modified aramides from aromatic dicarboxylic acids and aromatic diamines containing ether linkages was also reported.

Regarding the DSSP mechanism, polymerization is considered to follow the nucleation and growth model, according to well-known principles of solid state chemistry.[20–23,31] During the initial stages of salts DSSP, the volatile diamine component, can escape, e.g., hexamethylenediamine (HMD), as it has been observed for the cases of PA66 and 610 salts and also of different aromatic polyamide salts.[39–41] In a study of Papaspyrides *et al.*,[40] the diamine loss was proven to precede the water formation in the case of PA 66, resulting in defective surfaces on the salt crystal and thus creating active reaction centers. Following nucleation, the DSSP reaches a growth stage. Especially at high reaction temperatures, a transition from solid to melt state has been observed. This melting phenomenon has been explained by Papaspyrides *et al.*[10,11,20,27,30] by the formation of lower melting hydrated regions, formed by the accumulation of the by-product (water).

Among the studied DSSP examples, that of tetramethylenediammonium-terephthalate (4T salt) has not yet been examined (Figure 1), despite the fact that the relevant polyamide poly(tetramethylene terephthalamide) (PA 4T) presents increased interest in terms of properties and performance. It is a semicrystalline polyamide with a melting point around 430°C[13,16] and it cannot be polymerized directly from tetramethylenediamine (TMD) and terephthalic acid either by a melt or a solution technique. One problem is the temperature-favored acid catalyzed cyclization of TMD to mono-functional pyrrolidine (PRD) and ammonia (NH_3). Especially PRD can act as a chain terminator.[13] Another problem relates to the high melting point of PA4T, which is inside the thermal degradation temperature window.[16] The development of a DSSP technology can be considered as an interesting and promising route for the production of high quality PA 4T, restricting side reactions and thermal degradation in the polymer during its production.

Regarding the gas atmosphere, two existing approaches were considered in the current work for applying DSSP on 4T salt: (i) heating under continuous inert gas flow (open system), where water removal and the inertizing of the reactor are ensured at atmospheric pressure,[42] (ii) heating in an inert gas atmosphere (closed system) under overpressure, where the loss of monomers, oligomers, and by-product is hindered[41]; the pressure of the reactor gradually increases (autogenous system) due to water formation. To promote conversion, in a second step the pressure is released. After reaching atmospheric conditions, the reactor is flushed by passing a stream of inert gas through the system (1st approach).[40,43] The autogenous method provides a means of keeping the diamine monomers in the

reactor, while providing effective removal of water in the second step in order to favour conversion. Particularly in the 4T salt case however, the latter approach cannot be successfully applied due to chemical instability of TMD.

A thermogravimetric analysis (TGA) instrument was used as a micro-scale DSSP reactor, in order to exclude heat and mass transfer limitations. The DSSP progress was evaluated by continuous monitoring of the weight loss of the reacting mass, which is correlated to the conversion to polymer via the release of water. In addition, some diamine is also lost.[40,44] Reaction temperature (T_{DSSP}), heating rate to the reaction temperature (HR), and size of the opening in the reactor lid were systematically varied and derived products were analyzed. From the results obtained, the objective is to define a DSSP polycondensation mechanism of the 4T salt, suitable for proposing a scaled-up DSSP process valid for a range of terephthalamide salts.

EXPERIMENTAL PROCEDURE

Materials

Two morphologically different 4T salt grades were used as starting materials for the DSSP reactions. **Salt 1**, received in the form of fine powder, was prepared as described in previous work of our group[42] and was kindly provided by DSM Ahead B.V. **Salt 2** was crystallized from an aqueous solution and was precipitated in the form of thick rectangular crystals by cooling. SEM micro-photos on the herein used salts (Figure 2) reveal that **salt 1** consists of irregular particles of at most 0.3 × 0.2 mm^2, while the dimensions of the single crystals of **salt 2** were estimated at 3 × 4 mm^2. Thermal and analytical characteristics of the particular monomers, as determined by TGA/DSC analysis and titrations, are given in Table I and Figure 3. Polyamide 66 salt was used as a reference material and is a commercial grade by BASF (AH salz).

DSSP Runs

DSSP runs were carried out in a Mettler Toledo TGA/DSC 1 HT instrument, using 40 μL aluminum crucibles and nitrogen as carrier gas, controlled to a flow rate of 25 mL min^{-1}. About 15 mg of dried 4T salt was placed in the crucible, which was covered with a lid. The lid had a hole of either 50 μm or 2 mm on top. The samples were inserted into the TGA chamber at 30°C (T_0), preheated to 150°C (T_1) at a rate (HR) of 15°C min^{-1} and further heated up to (T_{DSSP}) with several HRs ranging from 0.5 to 20°C min^{-1}. Finally, an additional isothermal step at T_{DSSP} was applied for periods from 3 to 23 h. After

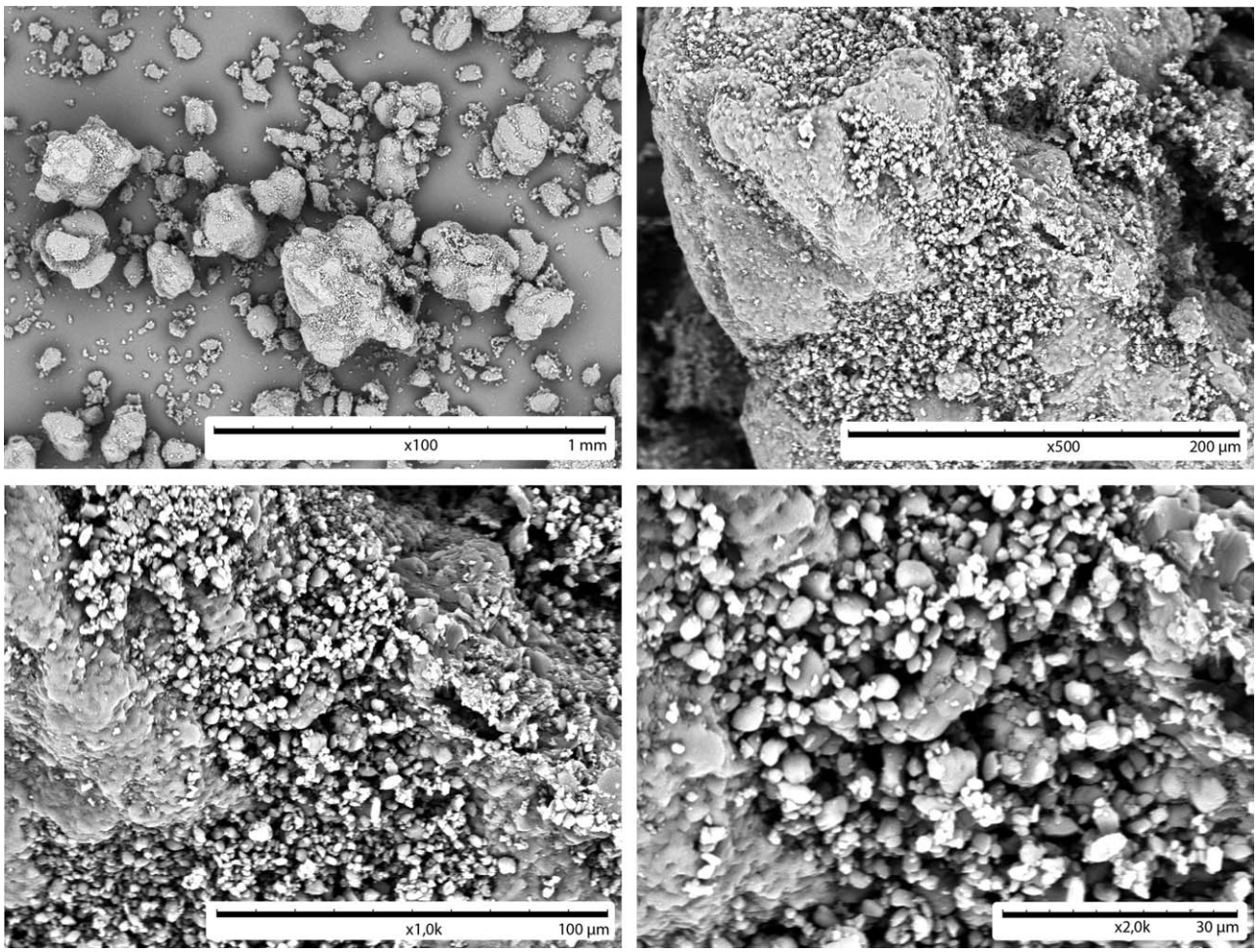

Figure 2. Morphology of 4T salts as observed by SEM. (a) Salt 1, (b) Salt 2.

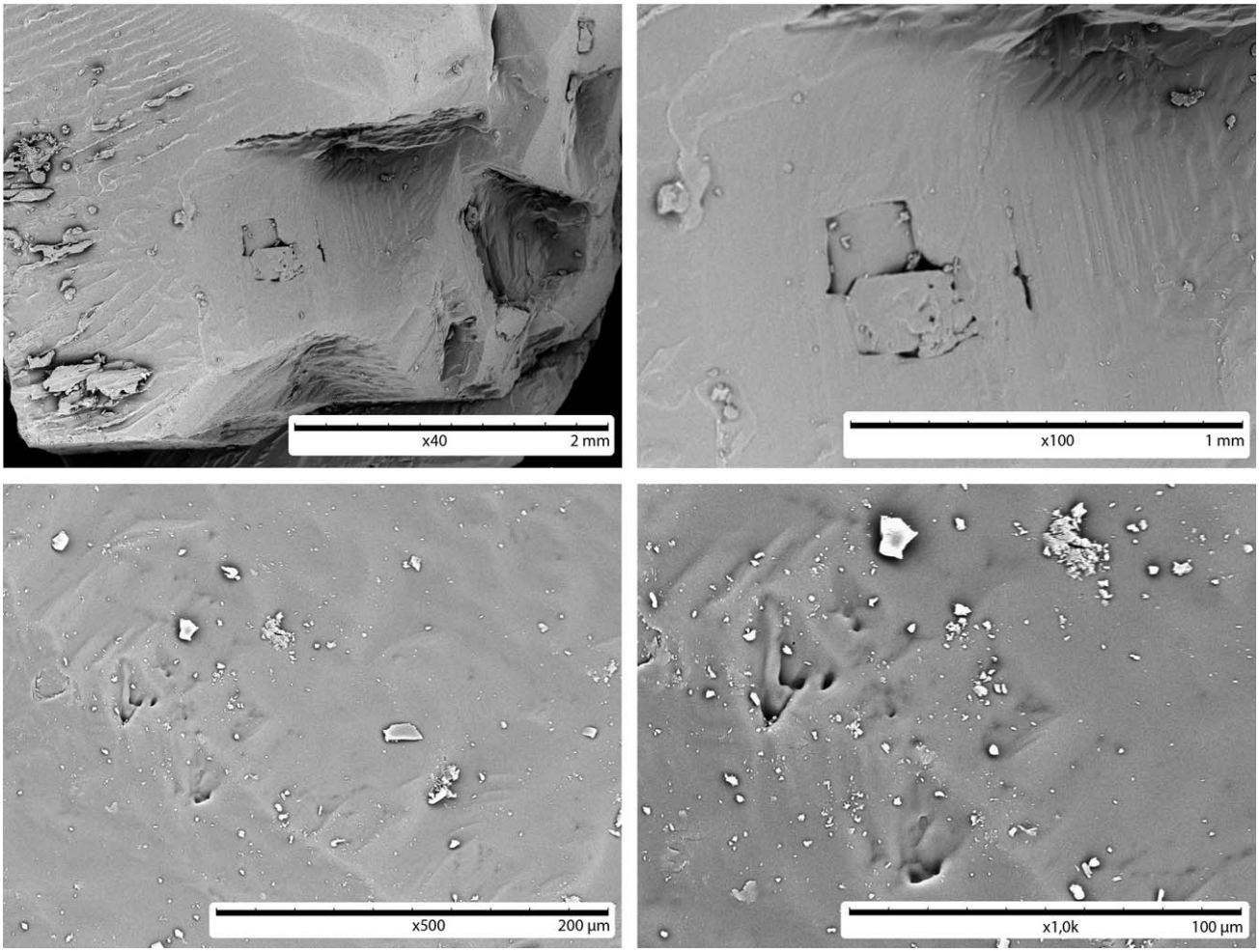

Figure 2. Continued.

the isothermal step the material was cooled almost instantaneously to room temperature.

TGA/DSC Analysis

Coupled TGA/DSC measurements on both the 4T salt grades and their derived PA4T products were carried out in a Mettler Toledo TGA/DSC 1 HT instrument. Nearly 4–6 mg of salt or polymer were placed in 40 μL aluminum crucibles and were sealed with a lid having a hole on top. The 4T salts were heated from 30 to 530°C with 10°C min^{-1}, while polyamide products were heated from 30 to 550°C with 20°C min^{-1}. In both cases nitrogen flow was controlled at 25 mL min^{-1}.

^{1}H NMR Analysis

^{1}H NMR spectra were received in a Bruker Advance 500 MHz instrument and the solvent used was deuterated sulfuric acid (D_2SO_4). In a typical spectrum of a PA4T sample, all characteristic peaks can be assigned to hydrogen atoms in the polymer chain and in the polymer end groups. This is shown with corresponding numbers in Figure 4. To calculate the number average molecular weight ($\overline{M_n}$), only the end groups are taken into account, including [−PRD] and $[-\mathrm{COOH}]_{TA}$, i.e., $\overline{M_n} = \frac{2x10^6}{[-NH_2]+[-COOH]+[-PRD]+[-COOH]_{TA}}$. End group concentrations are calculated by the end group signal intensities relative to the signal intensities of the polymer backbone and a detailed example of the calculations used herein is given in Table II.

SEM Microscopy

Scanning electron microscopy (SEM) was performed with a Hitachi Tabletop TM3000 microscope, with distance measuring capability. The microscope is equipped with a high-sensitivity

Table I. Thermal and Analytical Properties of 4T Salts

4T salt grades	T_m (°C)	ΔH_f (J g^{-1})	T_d (°C)	[—NH_2] (meq kg^{-1})	[—COOH] (meq kg^{-1})
Salt 1	287.5	524.3	287.9	7950	7950
Salt 2	298.7	532.7	299.8	7865	7868

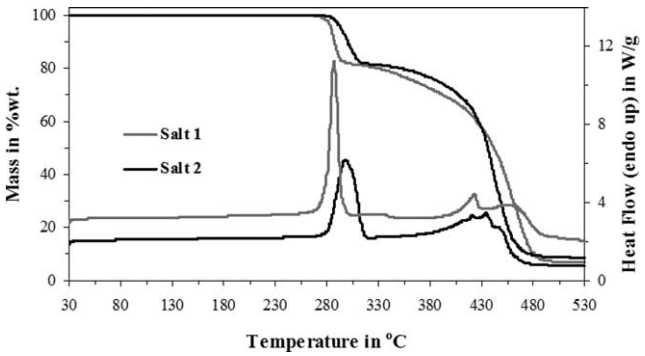

Figure 3. Coupled TGA/DSC curves of 4T salt grades 1 and 2, scanned from 30 to 530°C with 10°C min^{-1}.

semiconductor BSE detector, and operated at 15 kV on the filament. Samples were coated with a Au/Pd coating using a Quorum Technologies SC7620 sputter coater with a sputtering time of 150 seconds at a current of 10 mA.

RESULTS AND DISCUSSION

Semi-aromatic polyamide salts containing terephthalic acid (TA), and in particular 4T salt, exhibit a distinct thermal behavior as explained in another article of our group.[43] More specifically, a comparative DSC measurement (Figure 5) between a commercial 66 salt grade and 4T salt reveals this particular special melting behavior of TA-based polyamide salts.

Accordingly, 66 salt (Figure 5) shows a sharp endotherm peak at 203.1°C during DSC heating, which corresponds to the actual melting of the particular salt crystal. By integrating the area below the specific endotherm, energy absorption of 252 J g^{-1} was recorded. Subsequently at 216.6°C another endotherm is observed which is related to the melt polymerization reaction of the salt. This was further supported by the enthalpy value of 307 J g^{-1} which corresponds well with the heat of vaporization of water at atmospheric pressure, which is calculated as 310 J g^{-1} per g 66 salt when fully converted to PA66 and water. Therefore, it becomes evident that in the case of aliphatic salts, like 66 salt, the crystal first melts and then reacts to polymer. Nevertheless, both phenomena are clearly separated in time and show a total enthalpy value of 559 J g^{-1}.

On the contrary, in the case of 4T salt (Figure 5) only one endotherm at 287.5°C was observed, with an enthalpy value of 587 J g^{-1}. Further, the polymer was retrieved from the crucible without visible signs of melting. Therefore, it can be concluded that in the case of TA-based salts the endotherm in the DSC curve includes destruction of the salt crystal structure, polymerization, water evaporation, crystallization of the formed polymer, which all occur simultaneously.

A DSSP procedure and the pertinent reaction parameters for polymerizing 4T are examined below:

Defining the Proper Reaction Temperature Zone

Based on Figure 3, an endotherm peak was observed at 287.5°C for Salt 1, while the onset of the respective mass loss (T_{onset}), which matches with the onset of the DSC peak, was found at 285.9°C. Considering also that the monomers used are usually characterized by high sensitivity to reaction temperature variation and in order to inhibit any possible degradation or transition to the melt state,[38,45] the reaction DSSP temperature zone was arbitrarily selected at about 30–40°C below T_{onset} (T_{DSSP} = 250–260°C).

The Effect of Covering the Crucible

Based on the above hypothesis regarding the reaction temperature, two different 4T samples of **salt 1** were polymerized isothermally for 3 h at T_{DSSP} = 260°C in the TGA chamber, by preheating from 150 to 260°C with 1.3°C min^{-1}, mimicking heating rates of large-scale equipment. In the first experiment, the crucible was covered with a lid having a 2-mm diameter

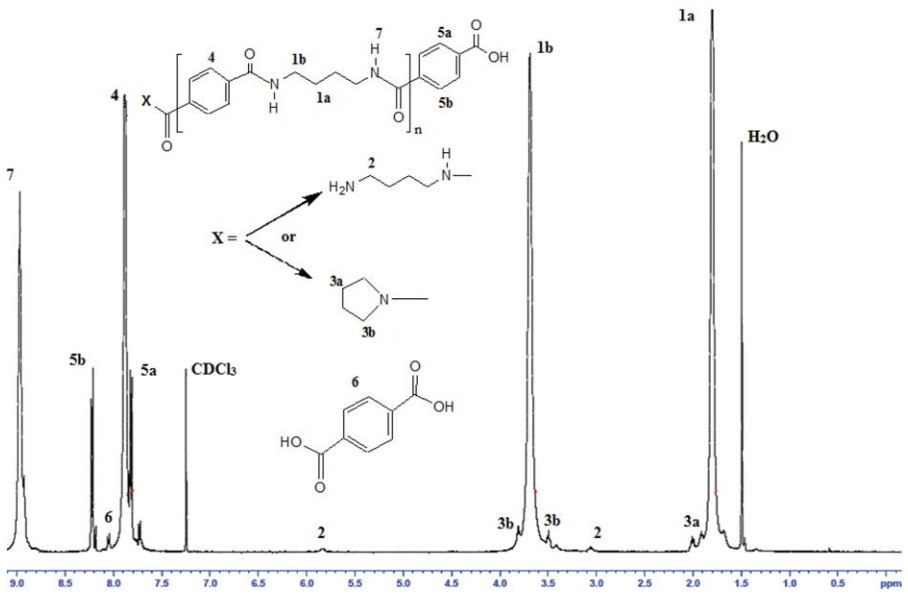

Figure 4. ^{1}H NMR spectrum of PA4T with interpretation of the peaks. [Color figure can be viewed in the online issue, which is available at wileyonlinelibrary.com.]

Table II. End-group Determination from ^{1}H NMR Spectra of PA4T Products Derived from Salt 1 and 2

	End—groups				$\overline{M_n}$[a] calculated by end-groups
	[—COOH]$_{TA}$	[—COOH]	[—NH$_2$]	[—PRD]	
PA4T samples	meq kg^{-1}	meq kg^{-1}	meq kg^{-1}	meq kg^{-1}	g mol^{-1}
4T 1 50 μm	48	762	29	227	1876
4T 1 2 mm	75	934	13	154	1701
4T 2 50 μm	29	758	45	170	1996
4T 2 2 mm	466	884	31	132	1322

$\overline{M_n}$ is calculated from the equation $\overline{M_n} = \frac{2x10^6}{[-NH_2]+[-COOH]+[-PRD]+[-COOH]_{TA}}$.

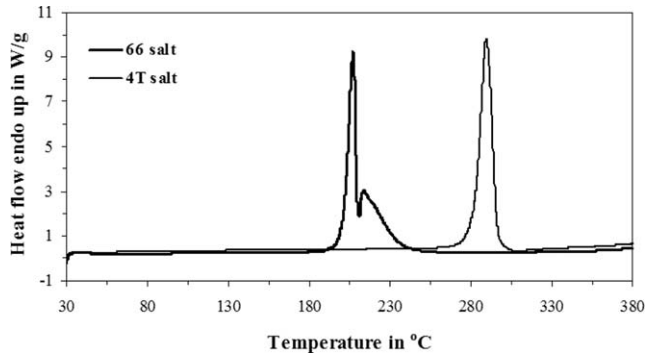

Figure 5. DSC curves of 66 and 4T polyamide salts scanned from 30 to 380°C with 10°C min^{-1}.

hole, while in the second experiment the hole in the lid had a diameter of just 50 μm (Figure 6). It seems that the lower diameter hole in the lid resulted in reducing the total mass loss at the end of the reaction ($t = 273$ min) from 18.1 to 15.6 wt % under otherwise identical conditions. Both samples however exceed the theoretical mass loss of 4T salt (14.2 wt %) by 1.4 and 3.9 wt %, respectively, indicating that apart from water, some volatile TMD ($T_b^0 = 158$°C) also escaped. These mass loss values can be translated to 159 and 443 mmol TMD per kg of salt for 50 μm and 2 mm holes, respectively, indicating that in both cases an excess of acid end-groups should be expected, which should be higher for the 2-mm crucible case.

Besides the apparent difference in TMD loss, also a difference in the slope of the two TGA curves is observed, continuing during the last hour of the DSSP process, when conversion is practically completed (Figure 6). For Salt 1, the TGA curve for the crucible with the 50-μm hole, reached a constant plateau after $t = 170$ min, while in the respective 2-mm hole case the mass decreased continuously already from $t = 150$ min. Assuming that this continuing mass loss is related to the thermal stability of the polymer formed, it seems that the slower reacting system polymerized in the covered cup, has almost eight times higher thermal stability, since the calculated slopes are 8×10^{-4} wt % min^{-1} and 6.3×10^{-3} wt % min^{-1} for 50 μm and 2 mm holes, respectively.

Furthermore, in the 2 mm case the reaction proceeds with 128% higher speed compared to the 50 μm case, since $t_{1/2}$, i.e. the time at T_{DSSP} required to reach 50% of conversion, was calculated at 15.4 and 35.2 min, respectively. A possible explanation for this phenomenon is that the vapor inside the crucible with the 50-μm hole was more slowly refreshed than in the 2-mm cup, leading to a more enriched atmosphere of TMD vapor thus delaying the DSSP initiation. In contrast, in the 2-mm case, the formed TMD vapor is immediately swept away by the nitrogen stream of the TGA chamber, thereby lowering the TMD and water vapor pressure. Thus, a TMD vapor seems to stabilize the 4T crystals and delay their reaction to polymer, which starts with the destruction of crystals (nucleation stage). Such stabilizing effects of volatile solvents surrounding a crystal, when the same solvent is part of the crystal structure are generally known by single crystal crystallographers.

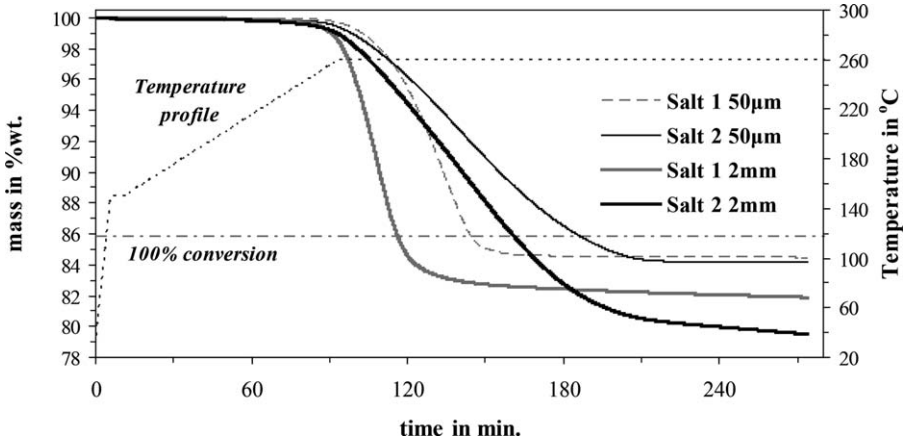

Figure 6. TGA curves of DSSP reaction of 4T salt. Comparative curves between different salts and 50 μm or 2 mm lid holes.

Table III. Calculations of End Group Concentration from ^{1}H NMR Spectra

Peaks	Formulas	*Molar mass (M) (g mol^{-1})	*H*	Shift (ppm)	Intensity (*I*)	$m = M^*I/H$ (g)	(1000*$m/m_{tot.}$)/ M (mol kg^{-1})	End groups (meq kg^{-1})
2		87.15	2	3.07	0.19	8.28	0.029	29
3a	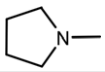	70.15	2	2.01	1.46	51.38	0.227	227
4	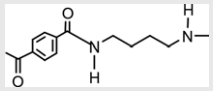	132.16 + 86.15 = 218.30	4	7.88	56	2787.69	3.957	-
5a	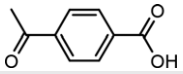	149.14	2	7.81	4.92	366.88	0.762	762
6	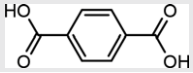	166.13	4	8.18	0.31	12.88	0.024	48
		Total mass ($m_{tot.}$)				3227	Total end groups	1066
	*MW_{TA} = 166.13	*MW_{TMD} = 88.15		*MW_{PRD} = 71.15			$\overline{M_n}$ (g mol^{-1})	1876

Example given for sample 4T 1 50 μm.

In addition, ^{1}H NMR analysis on the obtained PA4T products used in order to verify the hypotheses and conclusions are drawn from the aforementioned TGA data. Because of the high accuracy obtained with only tiny samples of 5–10 mg, ^{1}H NMR is especially well suited for determining the chemical composition of the polyamides produced in a TGA reactor, since these typically hold samples of 15 mg. Other analytical techniques, like potentiometric titrations and/or solution viscosity determination generally require several grams of material.

The analytical data (Table III) calculated from the ^{1}H NMR spectra are completely in line with the assumptions made from the TGA data above, and indicate that $\overline{M_n}$ values range from 1300 to 2000 g mol^{-1} and are dependent on process parameters as explained below. More specifically, the samples polymerized in the crucible with the 2-mm hole show about 18.5% higher acid end groups and about 55% lower amine ends than the respective samples from the crucible with the 50-μm hole, verifying that way that the difference in mass loss determined by the TGA was correctly attributed to the higher TMD loss. In addition, the samples from the cup with the 50-μm hole, shows about 32% higher PRD content than the respective samples from the 2-mm one, as it was assumed above, further lowering the acid end-group content and offering a better thermal stability to the polymer. Free TA was found 36% increased for the sample delivered from the 2 mm case, created by the higher diamine loss. However, the situation is complicated by the fact that some free TA may also evaporate, even though it has a low vapor pressure (about 117 Pa at 260°C).[46] Based on the total overview of the chemical composition of the two materials, the calculated number average molecular weight ($\overline{M_n}$) is 9.3% higher for PA4T derived from the 50-μm case.

Finally, turning to the thermal properties of the derived PA4T products, the effect of the severe diamine loss is evident also in this case. Accordingly, (Figure 7, Table IV) the polyamide product from the 50-μm case, shows slightly higher values in T_m, ΔH_m, and T_d, but lower residue compared to the respective 2 mm case. The differences are insignificant in this case, but will be much more pronounced for the case of **salt 2** below. These data support aforementioned DSSP TGA and ^{1}H NMR results. Once more, it seems that when TMD loss is limited by

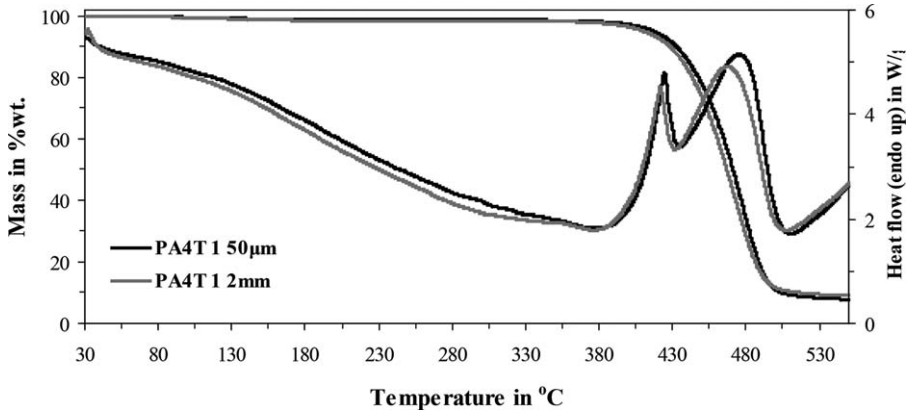

Figure 7. Coupled TGA/DSC scan on PA4T products of **salt 1** derived from 50 μm and 2 mm lid holes. (Scanned with 20°C min^{-1}).

Table IV. Thermal Properties of PA4T Products as Determined by Coupled TGA/DSC Measurements from 30 to 550°C with 20°C min^{-1}

PA4T samples	T_m (°C)	ΔH_m (J g^{-1})	T_d (°C)	Residue (wt %)
4T 1 50 μm	429.5	77.8	481.6	7.8
4T 1 2 mm	426.8	76.5	476.0	9.0
4T 2 50 μm	434.1	67.4	473.8	6.5
4T 2 2 mm	422.0	22.5	460.9	10.8

lowering the diameter of the hole in the lid, then a subsequent reduction of acid groups and/or free TA is achieved, resulting in better thermal properties and stability of the final polyamide material and reduced degradation side reactions.

The Effect of Salt Morphology

To further prove these first experimental observations considering **salt 1** and comprehend deeper into the mechanism of the DSSP of 4T salt, similar DSSP runs with varied hole diameters of the lids on crucibles were repeated for **salt 2**, which consists of much larger crystals (more than 10 times in diameter, Figure 2). The TGA curves of **salt 2** (Figure 6), show total mass loss values of 15.8 and 20.5 wt % for 50 μm and 2 mm cases, respectively. If the theoretical loss of reaction water of the 4T salt is subtracted from these values, then the calculated TMD loss is 203 and 824 mmol kg^{-1} of salt, meaning that the diamine loss is 44 and 381 mmol kg^{-1} higher than in the previous case of **salt 1**. Furthermore, regarding the thermal stability of the formed PA4T after $t = 210$ min, similar weight loss behavior with the DSSP of **salt 1** was observed. More specifically, the calculated slopes of the curves were 1.2×10^{-3} wt % min^{-1} and 1.44×10^{-2} wt % min^{-1} for the 50 μm and 2 mm cases, respectively, demonstrating that the formed PA4T gets 12 times more thermally stable only by limiting the hole in the lid of the crucible. However, this difference in thermal stability between the samples from 50 μm and 2 mm holes of the crucible of **salt 2** products is even higher than those of **salt 1** reported above, associated with the 86.5% higher diamine loss calculated in this case (i.e., salt **2**).

Turning to the rate of the DSSP reaction of **salt 2**, it seems that in both 50 μm and 2 mm lid holes, the speed is almost the same, since $t_{1/2}$ was calculated at 51.1 and 51.7 min, respectively. However, if we compare the $t_{1/2}$ values of the two different salts, the DSSP of **salt 2** proceeds 47 and 232% slower than **salt 1** for the 50 μm and 2 mm hole cases, respectively. This behavior can be attributed to a combination of two factors. On the one hand, **salt 2** shows about 11°C higher endotherm peak than **salt 1**, meaning that at the same T_{DSSP} (i.e., 260°C) the mobility of the end groups is lower for the case of **salt 2**, which also explains the higher diamine loss observed. On the other hand, the much larger particle size (or lower specific surface) of **salt 2** should inhibit the diffusion of water out of the system, delaying that way the reaction progress.

The difference in chemical composition, as determined by ^1H NMR analysis (Table III), of the two PA4T products derived by **salt 2** was more pronounced than in the respective cases of **salt 1** mainly due to the much higher TMD loss, which resulted in a high free TA content of about 4 wt % for the 2-mm case of salt 2. The highest acid group content leads to the lowest calculated $\overline{M_n}$ and also to the poorest thermal properties (Figure 8, Tables III and IV). In contrast, the sample with the crucible having a 50-μm hole of **salt 2** exhibits the highest amine ends content (45 meq kg^{-1}) and correspondingly the lowest total acid group content (787 meq kg^{-1}). In addition, PRD was 25% lower than the respective covered sample of **salt 1**, leading to a 6% higher $\overline{M_n}$. This implies that either the PRD formation is less for the case of **salt 2**, due to the stronger attachment of the diamine in a perfect salt crystal, or that PRD bounds easier to the higher specific surface of acid groups that the fine powder **salt 1** provides.

The Effect of Heating Rate

Based on the findings regarding the use of the lid, five different 4T salt samples of **salt 1** were polymerized isothermally at 260°C for 2 h in the TGA chamber with a lid with a 50-μm hole on top, but in this case were preheated from T_0 (e.g., 150°C) to the final T_{DSSP} (e.g., 260°C) with five different heating rates (HR) (e.g., 0.5, 1, 5, 10, and 20°C min^{-1}) as shown in Figure 9. The slopes of the TGA curves are parallel, indicating the same reaction mechanism, but this variation in HR results in a preheating stage lasting from 5.5 to 220 min. In addition, a slight difference of 0.25 wt % in mass loss was observed between 0.5 and 20°C min^{-1} preheating rates. This value seems low, but if the high reproducibility (i.e., deviation of 0.02 wt % in mass loss in five repeating runs) of the DSSP experiments in

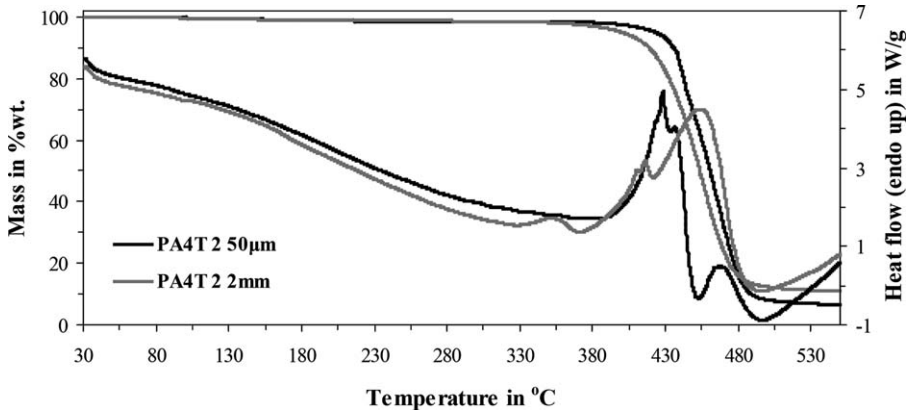

Figure 8. Coupled TGA/DSC scan on PA4T products of **salt 2** derived from 50 μm or 2 mm lid holes. (Scanned with 20°C min^{-1}).

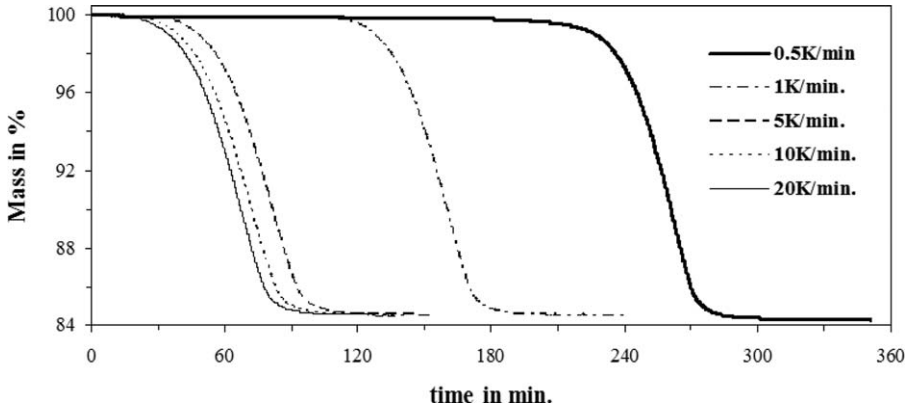

Figure 9. TGA curves of 4T salt polymerized with different HRs between T_0 and T_{DSSP}.

the TGA is taken into account, then it is understood that it is worthwhile mentioning. Moreover, ^{1}H NMR analysis on the derived PA4T samples reveals a clear correlation between the end-groups of the products and the applied HR (Figure 10). Accordingly, by increasing the HR from 0.5 to 20°C min^{-1}, [—NH_2] is increasing 18.6% while [—COOH] is decreasing by 4.3%. This should be expected, since by lowering the HR, the material is exposed to a temperature range where reaction rates are insignificant (e.g., 150–240°C) for a longer time, and volatile TMD is lost through evaporation and/or cyclization to PRD, leaving the remaining solid with an excess of acid groups. Consequently, in order to further restrict the TMD loss high HR should be applied. This is possible on the micro-scale of the TGA reactor, where accurate temperature control is achieved and heat and mass transfer limitations are virtually absent. However, in larger scale reactors (lab autoclaves, semi-pilot or plant reactors) HRs as high as 10 or 20°C min^{-1} cannot be applied. Therefore a HR of 1°C min^{-1} was used in subsequent experiments as a compromise between large and micro-scale capabilities.

Effect of Reaction Temperature

Following the above optimizations of the lid and the heating rate of the preheating stage, the effect of temperature on the DSSP of 4T salt was also evaluated. The 4T salt samples were polymerized isothermally, at five different temperatures i.e., 250, 252.5, 255, 257.5, and 260°C for 22, 14, 9, 6, and 2 h, respectively, (Figure 11). All five samples were preheated to 150°C (at 20°C min^{-1}) and then to each T_{DSSP} with a HR of 1°C min^{-1}. The initial time (t_0) of each experiment, is the time at which the experiment begins (30°C).

From the original TGA curves, plots of T_{DSSP} *vs.* $t_{1/2}$, total mass loss and TMD loss are presented in Figure 12. $t_{1/2}$ is defined as the time between reaching T_{DSSP} and the time at which 50% of conversion is reached. The total mass loss is compared to the theoretical loss of 4T salt (14.2 wt % in each case), and [—NH_2] loss is estimated as the amine end group deviation from the theoretical mass loss normalized in meq kg^{-1} of salt [i.e., $[—NH_2]_{loss} = 2000\times(m_f - m_{theor.})/88.15$], where m_f is the final mass loss of each experiment and $m_{theor.}$ is the theoretical mass loss of 4T salt (14.2 wt %). These three tools provide an indirect measure of the reaction progress. Accordingly, temperature seems to be the dominant parameter in the DSSP of 4T salt, since $t_{1/2}$ was increased from 74.4 to 675.5 min (ca., 900%) with a shift of 10°C in T_{DSSP} (from 260 to 250°C). Even with a smaller shift of 2.5°C (260°C to 257.5°C) an increase of 91 min (ca., 122%) in $t_{1/2}$ was observed. This is in line with the high thermal sensitivity of the DSSP observed in XT salts of longer aliphatic diamines reported by Volokhina *et al.*[34,44] However, total mass loss decreases by 5.6% from 260 to 250°C. This indicates that when the reaction proceeds at lower temperatures, less TMD evaporates, which is shown in the plot of [—NH_2] loss *vs.* T_{DSSP} (Figure 12). Accordingly, less TMD i.e. 379 vs.

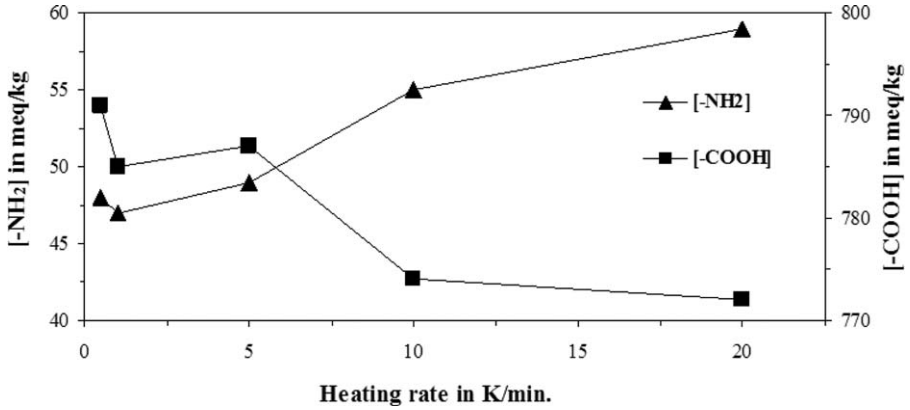

Figure 10. Plots of end-groups determined by ^{1}H NMR *vs.* HR between T_0 and T_{DSSP}.

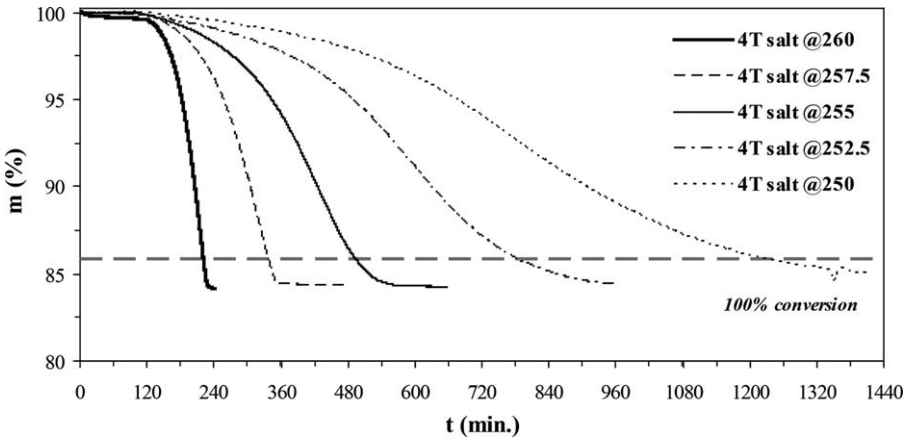

Figure 11. TGA curves of 4T salt polymerized at five different T_{DSSP}.

189 meq kg^{-1} was lost when T_{DSSP} was 10°C lower. However, this reduced TMD loss comes at a cost of 20 h of additional reaction time.

Furthermore, from the experimental DSSP data at five different temperatures, the estimation of kinetic parameters such as the activation energy (E_a) and pre-exponential factor (A) of 4T salt is also possible. Generally, the reaction rate of a chemical reaction (or a general kinetic model) is expressed through eq. (1)[47–49]:

$$\frac{da}{dt} = f(a)K(T) \tag{1}$$

where α is the conversion of the reaction or in the case of TGA data the normalized mass loss, calculated from the original data using eq. (2), where m_t is the mass recorded at any given time, m_i is the initial mass of salt and m_f *is* the final mass reached at the end of the end of the DSSP reaction.

$$a = \frac{m_i - m_t}{m_i - m_f} \tag{2}$$

In addition $f(\alpha)$ represents a temperature independent function of the mass loss and K(T) a function of temperature of the Arrhenius type,

$$\frac{da}{dt} = f(a)Ae^{-\frac{E}{RT}} \tag{3}$$

where A, E, T, and R are the pre-exponential factor, the activation energy (J mol^{-1}), the temperature in K, and the gas constant (8.314 J mol^{-1} K^{-1}), respectively. Hence, rate of change of conversion can be expressed as follows;

$$\frac{da}{dt} = f(a)Ae^{-\frac{E}{RT}} \tag{4}$$

A typical method suitable both for isothermal and dynamic experiments is that of Friedman[47] and when applied to eq. (4) the following is derived:

$$ln(^{da}/_{dt}) = ln(f(a)) + lnA - E/RT \tag{5}$$

Plotting ln($d\alpha/dt$) against 1/T, the slope yields the value of E/R for any given α. Figure 13 shows this plot for five different isothermal experiments. Consequently E can be calculated by multiplying the derived slope with the gas constant. The average calculated activation energy is equal to 535.2 kJ mol^{-1}, but the actual E values are shown in Table V and the variation of E with conversion is shown in Figure 14. This increasing trend of the activation energy values with conversion can be anticipated, since in DSSP the starting material is the salt containing the maximum possible number of end groups. As the reaction proceeds to higher conversions, the end groups are being consumed, leading to prepolymer intermediates of increasing chain length. In addition, this increasing dependence of E versus α, reveals also a reaction in which competitive phenomena occur.[52] Indeed this is valid in our case and in accordance with the herein proposed mechanism of the DSSP of 4T salt: Diamine

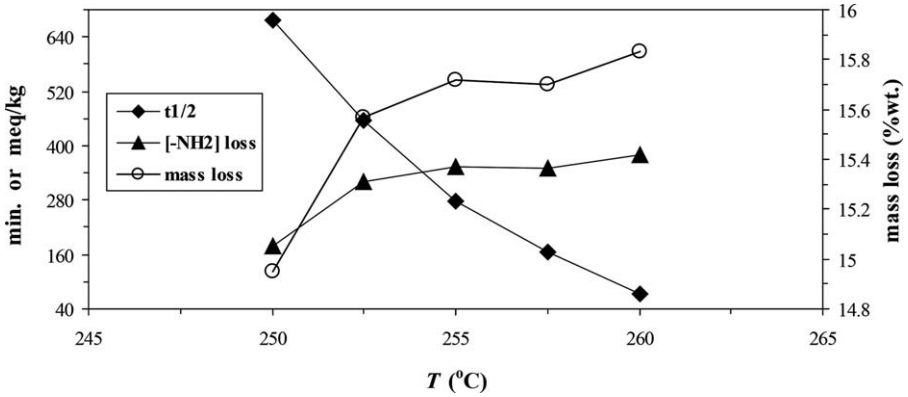

Figure 12. Calculated $t_{1/2}$, mass loss and TMD loss by TGA data of different DSSP temperatures.

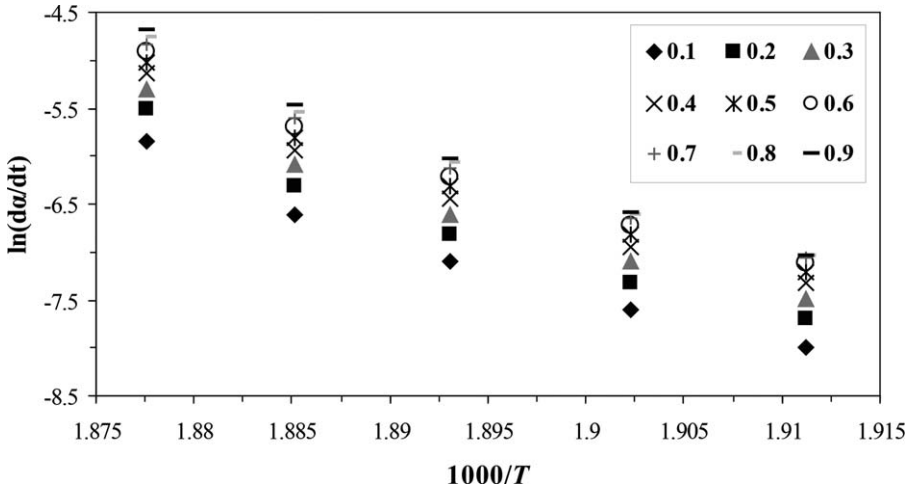

Figure 13. Friedman method, plots of $\ln(d\alpha/dt)$ *vs.* $1000/T$.

evaporation takes place in the beginning of the reaction creating nuclei, which constitute the active centers for promoting the reaction.[20,27,30,40] On the other hand, when the condensation begins, water is formed, which is also evaporated. These two phenomena can overlap, especially at low conversions (0–0.2), where Figure 14 shows a wide shoulder at low conversion.

Furthermore, in order to calculate the rest of the kinetic parameters, such as A and $K(T)$, it was assumed that the function $f(\alpha)$ is equal to 1-α, which fits the obtained TGA data best. Then eq. (5) becomes:

$$ln(^{da}/_{dt}) = [ln(1-a) + lnA] - E/RT \quad (6)$$

which allows the extraction of the pre-exponential factor from the intercept of the aforementioned linear plots. The obtained A values are also shown in Table V, and an average estimation is 6.789×10^{51}. Substituting the average values of A and E in eq. (3) we obtain the Arrhenius function $K(T)$ that describes the DSSP of 4T salt:

$$K(T) = 6.789 \times 10^{53} + e^{-64.367/T} \quad (7)$$

Total Assessment of DSSP Reaction of 4T Salt

In overall, the development of the DSSP process of 4T salt showed that part of the TMD was lost, since in all cases mass loss exceeded the theoretical one and all products have an excess of COOH over NH_2 groups. In fact, the herein results confirmed a previous work of Papaspyrides *et al.*,[35] where the loss of a less volatile diamine (HMD) preceded water formation and was found necessary in order to create defects on the salt crystal and thus initiate the DSSP reaction. Furthermore, through the herein suggested technique, the escaped TMD amount can be limited by adjusting the hole on the lid of the micro-reactor. Subsequently, this system was driven to complete conversion by an additional isothermal step at T_{DSSP}, and the quality of the PA4T formed was assessed satisfactory based by its thermal stability and lower COOH content. On the contrary, when the DSSP was performed with a 2-mm lid hole, the higher TMD loss resulted in higher COOH content. This resulted in low quality polyamide with reduced thermal stability.

Table V. Determination of Kinetic Parameters

α	E_a (kJ mol^{-1})	lnA	A
0.1	517.5	110.9	1.6×10^{42}
0.2	525.8	113.3	1.5×10^{45}
0.3	526.4	113.8	2.5×10^{45}
0.4	526.8	114.1	3.7×10^{45}
0.5	528.1	114.8	6.9×10^{45}
0.6	531.6	115.9	2.1×10^{43}
0.7	539.1	117.9	1.6×10^{39}
0.8	551.1	121.1	4.1×10^{50}
0.9	569.9	126.1	6.1×10^{46}
Average	535.2	116.4	6.8×10^{51}

Last but not least, another very interesting issue is that by applying this DSSP process on the 4T salt, the solid character of the final product is retained throughout the process and no transition to the melt is observed. This was evident macroscopically in all herein derived PA4T products, but also in the micro level as it is shown by SEM pictures (Figure 15). Accordingly, it is obvious that the individual 4T salt particles of both salt grades (Figure 2) retain their initial general morphology and do not show any agglomeration or sintering of the neighboring particles. In higher magnification (Figure 15), holes, cracks, and a slight quasi-melt transition could be noticed, but could be attributed to the paths that reaction water created in order to escape and are considered insignificant, since the outer particles remain in tact.

Summarizing, this work focused on developing a total DSSP process for the polymerization of 4T salt in the micro scale, through an alternative nonisothermal technique for the first time. Accordingly, unlike the typical isothermal DSSP processes, the herein described cycle, consists of three stages:

i. preheating the starting material from ambient temperature (i.e., $T_0 = 30$°C) to a temperature at which SSP is anticipated to have no influence on conversion (i.e., $T_1 = 150$°C), at a high rate (15°C min^{-1})

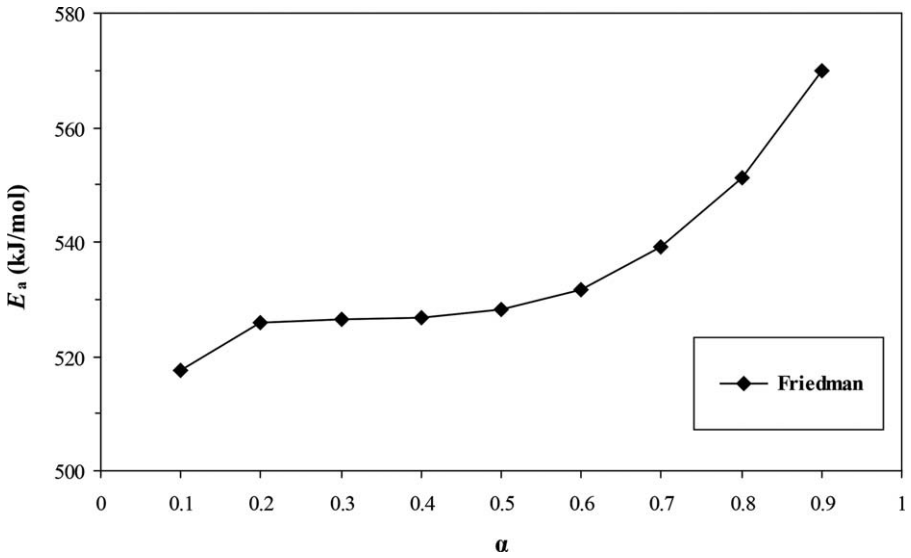

Figure 14. Variation of E_a versus the conversion (α), from isothermal experiments at five different temperatures.

ii. heating from T_1 to T_{DSSP} under the faster possible heating rate, in order to inhibit the formed TMD vapor to escape the system.
iii. heating the material isothermally at T_{DSSP}. To limit further TMD evaporation or cyclization, T_{DSSP} should be the lowest possible.

Following this uniform process and by adjusting the proper opening of the micro-reactor (i.e., crucible), polyamide 4T products can be received retaining their initial solid character throughout the polymerization course, avoiding thus completely

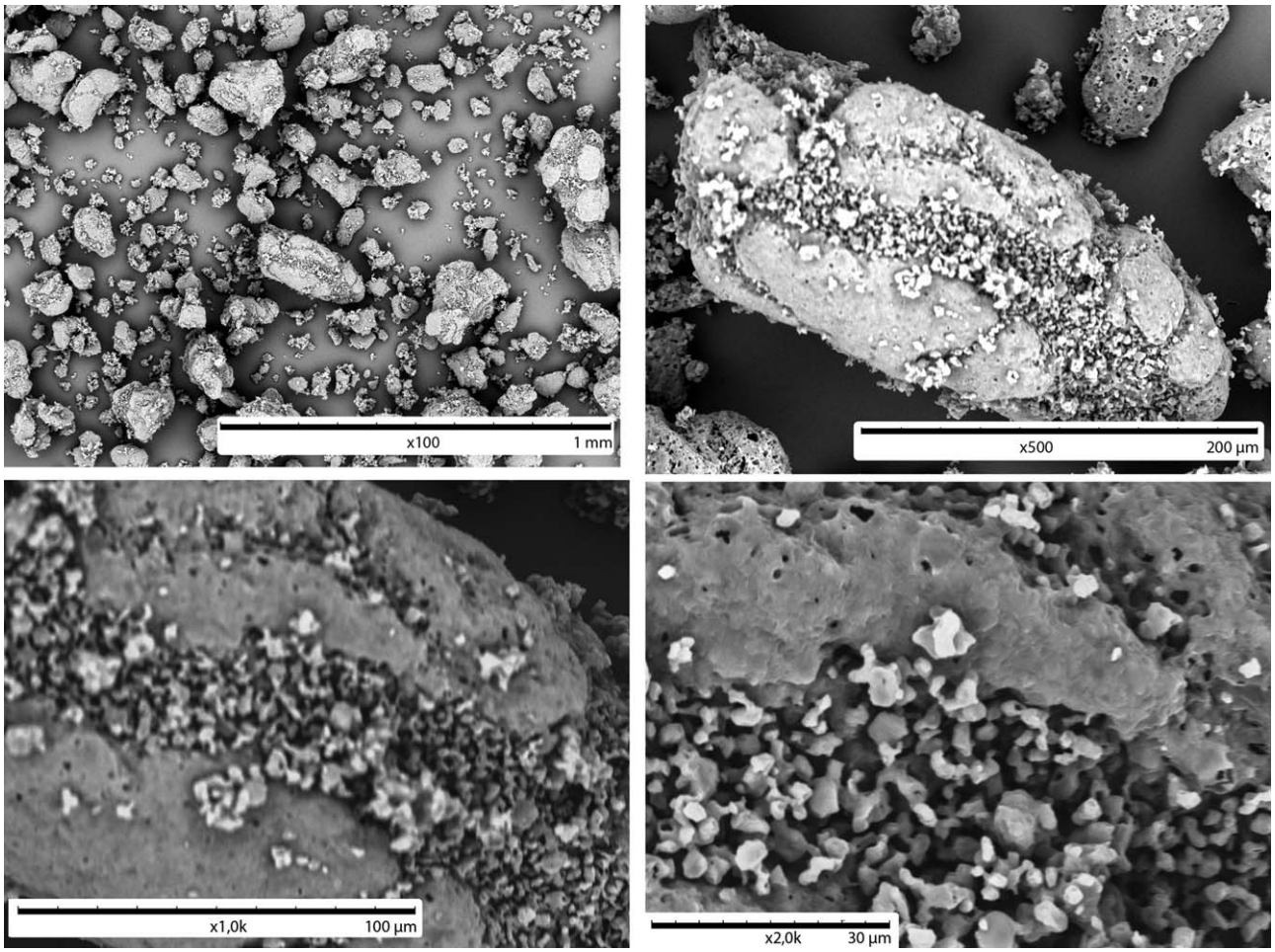

Figure 15. Morphology of PA4T products as observed by SEM. (a) PA4T from **salt 1**, (b) PA4T from **salt 2**.

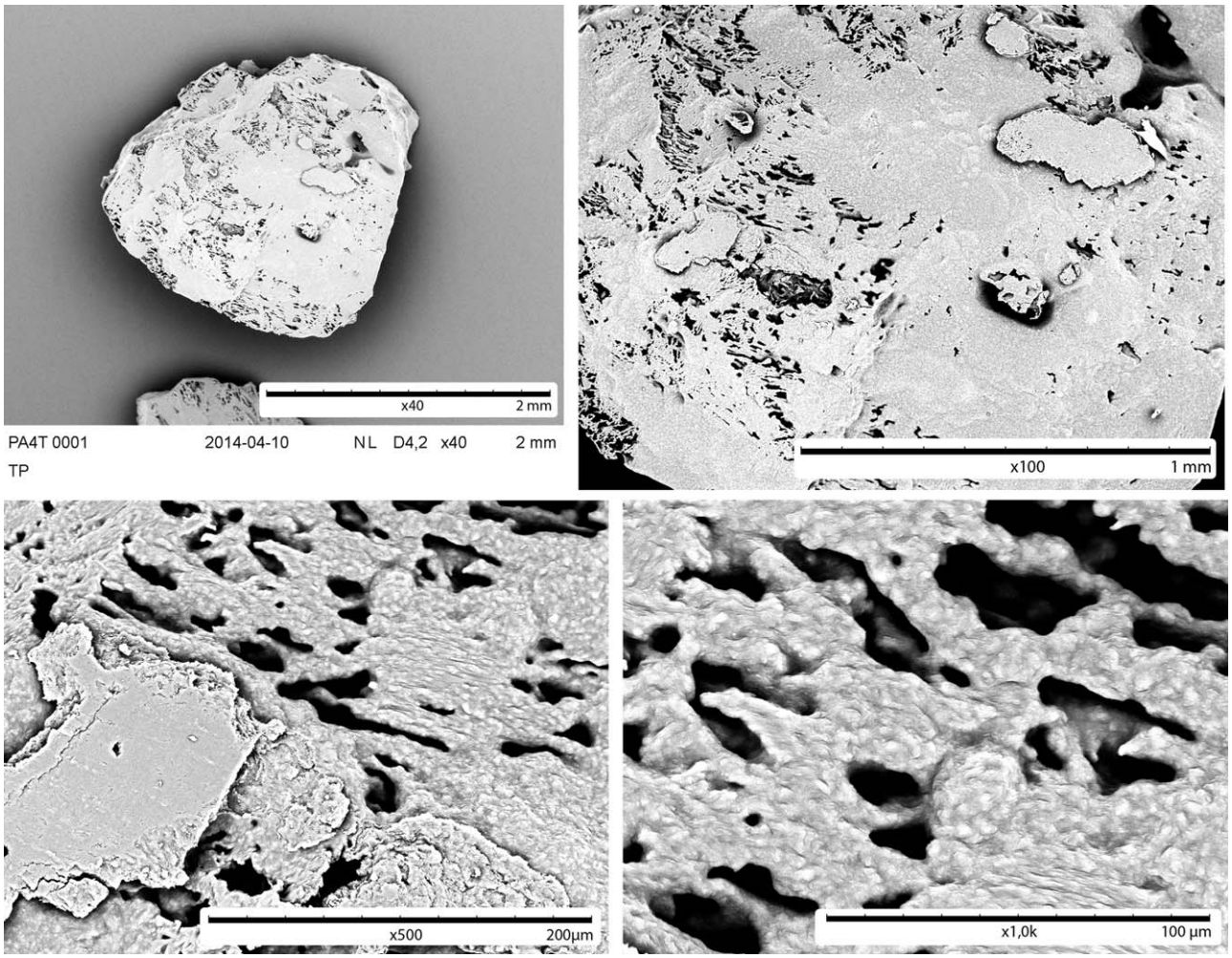

Figure 15. *Continued.*

any melt/solution prepolymerization step and operating under milder reaction conditions. Accordingly, the herein described DSSP process can be considered as a green technology, feasible even at larger than TGA scale for a variety of terephthalamides.

CONCLUSIONS

The aim of this work was to develop and optimize a direct solid state polymerization cycle (DSSP) of 4T salt in the micro scale of the TGA reactor, excluding completely any solution/melt prepolymerization step. More specifically, the DSSP procedure involved a preheating stage from ambient to reaction temperature with different heating rates and a final isothermal stage at the reaction temperature. As a result, mild conditions were applied and resulted in polyamide 4T grades with high polymerization rates and minimized thermal degradation, observed as residual isothermal mass loss after polymerization. A reaction mechanism was suggested, according to which the loss of the readily volatile TMD is creating defects on the surface of the salt crystal and thus accelerates the nucleation stage of DSSP. However, the quality of the end product is dependent on the TMD loss extent because it results in a high excess of carboxyl groups, which favors polyamide degradation reactions. The diamine loss can be limited through increasing the heating rate of the preheating step, limiting the vent size, and reducing the reaction temperature, resulting in final products of higher quality, however the inevitable temperature-favored cyclization of TMD to PRD inhibits a high molecular weight build up. The herein suggested DSSP cycle was proven feasible as a green polymerization technique for PA4T, and can be expanded to other semi-aromatic terephthalamides.

REFERENCES

1. Marchildon, K. *Macromol. React. Eng.* **2011**, *5*, 22.
2. Weber, J. Polyamides, General: Kirk-Othmer Encycl. Chem. Techn. Wiley: NJ, **1996**; p 1.
3. Korshak, V.; Frunze, T. Synthetic Heterochain Polyamides; IPST: Jerusaleum, **1964**.
4. Rulkens, R; Koning, C. In Polymer Science: A Comprehensive Reference; Matyjaszewski, K., Möller, M., Eds.; Elsevier BV: Amsterdam, **2012**, Vol. *5*, p 431.
5. Garcia, J.; Garcia, F.; Serna, F. *Progr. Polym. Sci.* **2010**, *35*, 623.
6. Gao, D.; Song, C.; Song, X.; Wang, X.; Wang, Y. Production Method of High-strength High Modulus PMIA Super-short Fiber; Yantai Spandex Co. Ltd; Chinese Patent, **2010**.

7. Ciu, X.; Li, L.; Li, X.; Peng, T.; Wang, F. Polyphenylene Terephthalamide Fiber and Preparation Method Thereof; China Bluestar Chengrand Chemi; Chinese Patent, **2010**.
8. Zhang, G.; Yang, H.-W.; Zhang, S.-X.; Zhang, Y.; Wang, X.-J.; Yang, J. *J. Macrom. Sci. A: Pure Appl. Chem.* **2012**, *49*, 414.
9. Novitsky, T.; Lange, C.; Mathias, L.; Osborn, S.; Ayotte, R.; Manning, S. *Polymer* **2010**, *51*, 2417.
10. Vouyiouka, S.; Karakatsani, E.; Papaspyrides, C. *Prog. Polym. Sci.* **2005**, *30*, 10.
11. Papaspyrides, C.; Vouyiouka, S.; Eds. Solid State Polymerization. Wiley: New Jersy, **2009**.
12. Vouyiouka, S.; Papaspyrides, C. Encyclopedia of Polymer Science and Technology, 4th ed.; Wiley: New Jersey, **2011**; p 1.
13. Gaymans, R. *J. Polym. Sci. A: Polym. Chem* **1985**, *23*, 1599.
14. Gaymans, R.; Van der Ham, A. *Polymer* **1984**, *25*, 1755.
15. Gaymans, R.; Aalto, S. *J. Polym. Sci. A Polym. Chem.* **1989**, *27*, 423.
16. Rulkens, R.; Crombach, R. Tetramethylene Terephthalamide and Hexamethylene Terephthalamide-based Copolyamides and Their Preparation; WO2001025311A1, **2001**.
17. Roerdink, E.; Warnier, J. Polyamides with Improved Melt Stability; EP411709A1, **1991**.
18. Rulkens, R.; Crombach, R. Heat-resistant Semi-crystalline Semi-aromatic Polyamide; WO2007085406A1, **2007**.
19. Kim, Y.; Yohana, K.; Lee, H.; Kim, J. *Ind. Eng. Chem. Res.* **2012**, *51*, 15801.
20. Papaspyrides, C.; Kampouris, E. *Polymer* **1984**, *25*, 791.
21. Kampouris, E.; Papaspyrides, C. *Polymer* **1985**, *26*, 413.
22. Papaspyrides, C.; Kampouris, E. *Polymer* **1986**, *27*, 1437.
23. Papaspyrides, C. *Polym. Int.* **1992**, *29*, 293.
24. Grabar, D.; Hsia, C.; Catherine, S. *J. Polym. Sci. C* **1963**, *3*, 105.
25. Frayer, P.; Lando, J. *Mol. Cryst. Liq. Cryst.* **1969**, *A1*, 465.
26. Katsikopoulos, P.; Papaspyrides, C. *J. Polym. Sci. A Polym. Chem.* **1994**, *32*, 451.
27. Papaspyrides, C. *Polymer* **1990**, *31*, 490.
28. Ikawa, T. In: The Polymeric Materials Encyclopedia; Salamone, J. C., Ed.; CRC Press: Boca Raton, FL, **1996**; Vol. *6*, p 4689.
29. Ikawa, T. In Solid State Polymerization; Papaspyrides, C.; Vouyiouka, S.; Eds. Wiley: New Jersey, **2009**; Chapter 6, 179–197.
30. Papaspyrides, C. *Polymer* **1988**, *29*, 114.
31. Vouyiouka, S.; Papaspyrides, C. In: Comprehensive Polymer Science; Matyjaszewski, K., Moeller, M., Ed.; Elsevier: Athens, **2012**; Vol. *4*, p 857.
32. Yamazaki, T.; Kaji, K.; Kitamaru, R. *Bull. Kyoto Univ. Educ. Ser. B* **1983**, *63*, 53.
33. Macchi, E.; Giorgi, A. *Makromol. Chem.* **1979**, *180*, 1603.
34. Volokhina, A.; Kudryavtsev, G.; Skuratov, S.; Bonetskaya, A. *J. Polym. Sci.* **1961**, *53*, 289.
35. Bizzarri, P.; Della Casa, C.; Monaco, A. *Polymer* **1981**, *22*, 1263.
36. Bizzarri, P.; Della Casa, C.; Monaco, A. *Polymer* **1980**, *21*, 1065.
37. Iwakura, Y.; Uno, K.; Chau, N. *J. Polym. Sci. Polym. Chem. Ed.* **1973**, *11*, 2391.
38. Shoji, Y.; Mizoguchi, K.; Ueda, M. *Polym. J.* **2008**, *40*, 680.
39. Khripkov, E.; Kharitonov, V.; Kudryavtsev, G. *Khim. Volokna* **1970**, *6*, 63.
40. Papaspyrides, C.; Vouyiouka, S.; Bletsos, I. *Polymer* **2006**, *47*, 1020.
41. Oya, S.; Tomioka, M.; Araki, T. *Kobunshi Kagaku* **1966**, *23*, 415.
42. Porfyris, A. D.; Vouyiouka, S. N.; Papaspyrides, C. D.; Rulkens, R.; Grolman, E.; Poel, G. V. Investigating Alternative Routes for Semi-aromatic Polyamide Salt Preparation in press *J. Appl. Polym. Sci.* **2016**, DOI: 10.1002/APP.42987
43. Wlloth, F. Solid State Preparation of Polyamides (Vereinigte Glasstoff-Fabriken A.G.). US Patent 3,379,696, **1968**.
44. Volokhina, A.; Kudryavstev, G.; Raeva, M.; Bogdanov, M.; Kalmykova, V.; Mandrosova, F.; Okromchedidze, N. *Khim. Volokna* **1964**, *6*, 30.
45. Gaymans, R.; Van Utteren, T.; Van Den Berg, J.; Schuyer, J. *J. Polym. Sci. Polym. Chem. Ed.* **1977**, *15*, 537.
46. Boussia, A.; Damianou, C.; Vouyiouka, S.; Papaspyrides, C. *J. Appl. Polym. Sci.* **2010**, *116*, 3291.
47. Popescu, C.; Segal, E. *Inc. Int. J. Chem. Kinet.* **1998**, *30*, 313.
48. Vyazovkin, S.; Burnham, A.; Criado, J.; Pérez-Maqueda, A.; Popescu, C.; Sbirrazzuoli, N. *Thermochim. Acta* **2011**, *520*, 1.
49. Shih-Fu, L.; Ming, C.; Chi He, C. *J. Appl. Polym. Sci.* **2012**, *123*, 3610.
50. Kosinski, L.; Soelch, R. Low Temperature Nylon Polymerization Process. US005665854A, **1997**.
51. Zeng, H.; Feng, L. *Gaofenzi Tongxun* **1983**, *5*, 321.
52. Vyazovkin, C.; Wight, A. *Annu. Rev. Phys. Chem.* **1997**, *48*, 125.